

The Influence of Linear Permanent Magnet Generator Sizing on the Techno-Economic Performance of a Wave Energy Converter

Tan, Jian; Wang, Xuezhou; Laguna, Antonio Jarquin; Polinder, Henk; Miedema, Sape

DOI

[10.1109/LDIA49489.2021.9505880](https://doi.org/10.1109/LDIA49489.2021.9505880)

Publication date

2021

Document Version

Final published version

Published in

Proceedings of the 13th International Symposium on Linear Drives for Industry Applications, LDIA 2021

Citation (APA)

Tan, J., Wang, X., Laguna, A. J., Polinder, H., & Miedema, S. (2021). The Influence of Linear Permanent Magnet Generator Sizing on the Techno-Economic Performance of a Wave Energy Converter. In *Proceedings of the 13th International Symposium on Linear Drives for Industry Applications, LDIA 2021* IEEE. <https://doi.org/10.1109/LDIA49489.2021.9505880>

Important note

To cite this publication, please use the final published version (if applicable).
Please check the document version above.

Copyright

Other than for strictly personal use, it is not permitted to download, forward or distribute the text or part of it, without the consent of the author(s) and/or copyright holder(s), unless the work is under an open content license such as Creative Commons.

Takedown policy

Please contact us and provide details if you believe this document breaches copyrights.
We will remove access to the work immediately and investigate your claim.

Green Open Access added to TU Delft Institutional Repository

'You share, we take care!' - Taverne project

<https://www.openaccess.nl/en/you-share-we-take-care>

Otherwise as indicated in the copyright section: the publisher is the copyright holder of this work and the author uses the Dutch legislation to make this work public.

The Influence of Linear Permanent Magnet Generator Sizing on the Techno-Economic Performance of a Wave Energy Converter

1st Jian Tan

Department of Maritime & Transport
Technology
Delft University of Technology
Delft, Netherlands
J.Tan-2@tudelft.nl

2nd Xuezhou Wang

Department of Maritime & Transport
Technology
Delft University of Technology
Delft, Netherlands
X.Wang-3@tudelft.nl

3rd Antonio Jarquin Laguna

Department of Maritime & Transport
Technology
Delft University of Technology
Delft, Netherlands
A.JarquinLaguna@tudelft.nl

4th Henk Polinder

Department of Maritime & Transport
Technology
Delft University of Technology
Delft, Netherlands
H.Polinder@tudelft.nl

5th Sape Miedema

Department of Maritime & Transport
Technology
Delft University of Technology
Delft, Netherlands
S.A.Miedema@tudelft.nl

Abstract—Downsizing the Power Take-off (PTO) rating has been proven to be beneficial for decreasing the Levelized Cost of Energy (LCOE) of wave energy converters (WECs). However, the linear permanent magnet (PM) generator has not yet been modelled and optimized in detail in previous feasibility studies. This paper extends the study of the PTO downsizing to further investigate the influence of the linear PM generator sizing on a WEC's techno-economic performance. The generator is sized for providing different maximum forces, and the effect of sizing on the generator performance is presented. The efficiency map of the selected linear generator design is applied to evaluate the annual energy production (AEP) and finally identify its influence on the techno-economic performance of a WEC.

Keywords—wave energy converter, linear permanent magnet generator, downsizing, techno-economic performance.

I. INTRODUCTION

Ocean waves have been investigated for decades due to their substantial renewable energy content, and over one hundred different types of WECs have been proposed or even tested [1]. However, the techno-economic indicators of WECs, such as their LCOE, are not competitive with other renewable technologies [2]. Our current work presents a collective sizing method for WECs, by which a heaving point absorber and PTO sizing can be implemented to reduce the LCOE [3]. It came to a conclusion that downsizing the PTO system was beneficial for reducing the system LCOE.

There are normally four categories of PTO systems under investigation. They are hydraulic, pneumatic, mechanic systems and linear generators [1], among which linear PM generators have received significant attention [4]–[8]. The main advantage of a linear PM generator is the reduced number of intermediate conversion steps which finally leads to a high conversion efficiency and reliability. Several prototypes equipped with the linear generator have been successfully designed and tested, such as the Archimedes Wave Swing (AWS) and the Uppsala university wave power concept [6], [9], [10]. However, there is limited literature addressing the influence of PTO sizing on the linear generator efficiency and finally techno-economic performance of WECs. On the one hand, the PTO sizing implies the physical limits like force, power and stroke constraints which actually

limit the maximum energy absorbed by WECs. On the other hand, for the linear PM generators, the PTO sizing also has an influence on their conversion efficiencies [11]. This last aspect has not yet been considered in our recent paper [3] where the PTO efficiency was assumed to be constant regardless of its size.

The contribution of this paper is to identify the impact of sizing on the generator efficiency and techno-economic performance of WECs with a linear PM generator. The paper starts with the description of the WEC concept and the linear PM generator reference. Then, a frequency domain model for hydrodynamic performance and an analytical model for generators are established to calculate the WEC performance. Rather than designing a complete new generator, the scaling principles are applied to estimate rough generator designs with respect to different PTO sizes. Then the effects of the PTO sizing on the generator efficiency, as well as the techno-economic performance of the WEC are analysed. Finally, conclusions are drawn.

II. CONCEPT DESCRIPTION

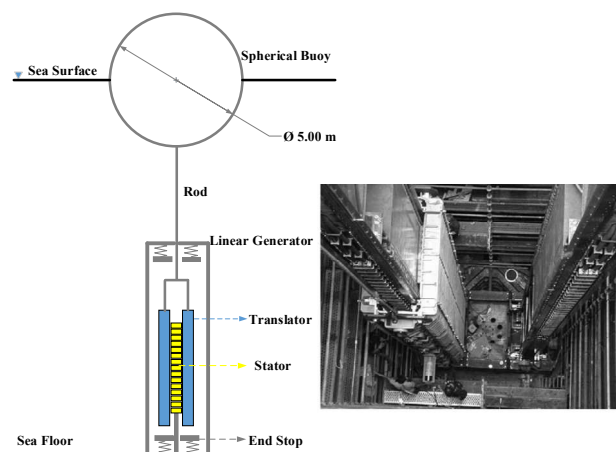


Fig. 1. Schematic of the heaving point absorber concept and photo of the reference generator in AWS pilot plant [4]

Fig. 1 shows the schematic of the studied heaving point absorber WEC system in which a linear generator operates as the PTO system. Fig. 1 also shows the photo of the reference linear PM generator that adopted and tested in AWS pilot

plant. The generator is bottom founded and its translator is connected to the floater by a rod. The floater is a sphere with a radius of 2.5 m. The draft of the floater is also 2.5 m. Excited by the incoming wave force, the floater moves up and down. The end stop devices are installed on both top and bottom of the generator to prevent the excessive motion.

The modelling and design of a linear PM generator, as well as the experimental validation and the full-scale sea trial in the AWS project was presented in [9], [12]. AWS was the first large-scale wave energy plant applying the linear PM generator in this research area.

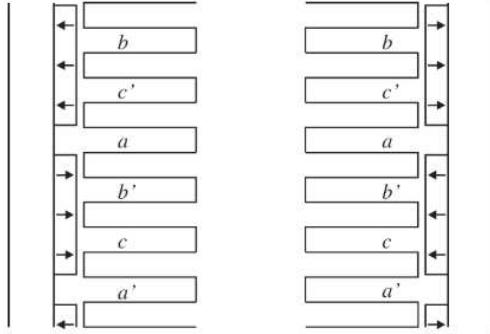


Fig. 2. Cross-section of a generator part in the AWS, in which a/a' , b/b' and c/c' are the current directions

Fig. 2 shows the cross-section of a three-phase generator. The generator is double sided to balance the attractive forces between the stator and translator [4]. The magnets are mounted on the translator segments and coils are wound on the stator segments. To reduce cost, the translator with the magnets is only slightly longer than the stator. This implies that the overlap between the stator and translator is partial during a large floater displacement. A back-to-back voltage source converter is used to vary the phase angle between no-load voltage and current.

TABLE I. SPECIFICATION OF THE REFERENCE GENERATOR

Parameter	Symbol	Reference machine
Rated power	P_{rated}	1 MW
Maximum force	F_{max}	900 kN
Maximum velocity	u_{max}	2.2 m/s
Stroke	S	7 m
Translator length	L_t	8 m
Stator length	L_s	5 m
Air gap	g	5 mm
Slot width	b_s	15 mm
Stack length	l_s	1 m
Magnet pole width	b_p	79 mm
Pole pitch	τ_p	0.1 m
Tooth width	b_t	19 mm
Number of conductors per slot	N_s	6

TABLE I gives some of the important parameters of the reference generator. The translator, stator, stack length and

pole pitch were defined in [9], and other parameters are taken from a direct-drive wind turbine generator design [13] which corresponds to a comparable maximum force and rated power with the reference generator in this work.

III. METHODOLOGY

A. Hydrodynamic Modelling of the Floater

The dynamic response of WECs in different wave states is calculated by frequency domain modelling. For convenience, the equation could be represented by complex amplitudes if the body is assumed to perform harmonic motion [14]. Therefore, according to Newton's second law, the motion of the WEC can be described as:

$$m\hat{a} = \hat{F}_{hs} + \hat{F}_e + \hat{F}_{pto} + \hat{F}_r \quad (1)$$

where m and a are the mass and acceleration of the oscillating body; F_{hs} , F_e , F_r and F_{pto} are the hydrostatic force, wave excitation force, wave radiation force and PTO force respectively. In this work, a linear passive PTO model is used to simulate the PTO behavior, giving

$$F_{pto} = -u(t)B_{pto} \quad (2)$$

where B_{pto} and u are the PTO damping coefficient and floater velocity. In order to obtain F_e and F_r , the excitation force, hydrodynamic damping and added mass coefficients are necessary. They are calculated by open source boundary element method (BEM) software Nemoh, and the results have been reported in [3]. Besides, the optimal PTO damping coefficient for each wave state and the given force and displacement constraints can be obtained by the method proposed in [3].

B. Generator Modelling

The analytical model has been proposed for calculating the performance of the linear PM generator of AWS, and the calculation has been validated by experimental measurements [12]. The model is adopted here to calculate the performance of different size generators. The effect of magnetic saturation is neglected here since it is not significant in most operating conditions for this linear generator design [7]. The necessary equations and explanations are presented in the following text, and more details can be found in [12].

The fundamental space harmonic of the magnetic flux density in the air gap due to the magnets is calculated as

$$\hat{B}_{gm} = \frac{l_m}{\mu_{rm}} B_{rm} \frac{4}{\pi} \sin\left(\frac{\pi b_p}{2\tau_p}\right) \quad (3)$$

where l_m is the magnet length in the magnetization direction, μ_{rm} is the recoil permeability of the magnets and B_{rm} is the remanent flux density of the magnets. The no-load phase voltage induced by this flux density in the stator winding is

$$E_p = \sqrt{2} p l_s N_s k_w v \hat{B}_{gm} \frac{l_{act}}{L_s} \quad (4)$$

where v is the floater velocity, p is the number of pole pairs, l_{act} is the actual length of the overlap between the stator and translator, and k_w is the winding factor. The stator phase resistance is calculated from the machine dimensions, the number of turns in a slot and the cross-section of a slot:

$$R_t = \rho_{Cu} \frac{I_{Cus}}{A_{Cus}} = \rho_{Cu} \frac{2N_s^2 (l_s + 2\tau_p)}{ph_s b_s k_{sfil}} \quad (5)$$

where ρ_{Cu} is the resistivity of copper, and k_{sfil} is the copper fill factor of the slots. The iron losses are calculated as

$$P_{Fes} = 2P_{Fes0} \left(m_{Fest} \left(\frac{b_s + b_t}{b_t} \right)^2 + m_{Fesy} \left(\frac{\tau_p}{\pi h_{sy}} \right)^2 \right) \frac{f_c}{f_0} \left(\frac{\hat{B}_{gm}}{B_0} \right)^2 \quad (6)$$

As the PTO damping coefficient is determined by the method proposed in [3], the required generator force F_{ge} can be calculated by (2). Then, the power taken by the generator windings is calculated as

$$P_{wd} = F_{ge} v - P_{Fes} \quad (7)$$

The current I_s can be divided into quadrature (or force making) component I_{sq} and direct (or flux making) component. The current I_s is initially assumed to be in phase with the no-load voltage E_p , which implies that there is no direct component as seen in the first phasor diagram in Fig. 3. To extract this power, the current can be calculated as

$$I_s = I_{sq} = \frac{P_{wd}}{mE_p} \quad (8)$$

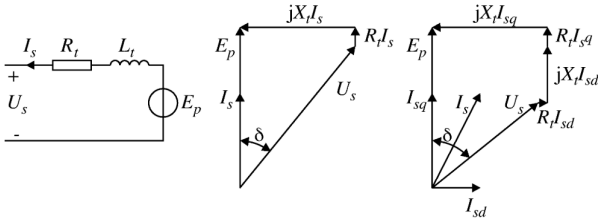


Fig. 3. Equivalent circuit of the generator and the phasor diagram with the converter.

If the current is larger than the maximum current of the converter I_{conm} , the current is limited to the maximum current. In this sense, the generator force is also reduced compared to the required generator force. Then, the terminal voltage can be calculated as

$$U_s = \sqrt{(E_p - I_{sq} R_t)^2 + (\omega_e L_t I_{sq})^2} \quad (9)$$

If the terminal voltage is larger than the rated converter voltage U_{conm} , the current also gets a direct component I_{sd} to make the terminal voltage equal to the rated converter voltage. This is shown in the second diagram in Fig. 3. If the resulted current under this condition is then larger than the maximum converter current, the operating point is then defined by the maximum converter current and the rated converter current. In these conditions, the actual generator force is less than the required generator force.

The converter losses are divided into three parts: 1) a small constant part, including power dissipated in power supplies, gate drivers, control, cooling systems among others; 2) a large part proportional to the current, including switching losses and conduction losses; 3) a part proportional to the current squared, including conduction losses [15]. For simplification, the converter losses are assumed to be only dependent on the generator side, and then they are calculated as

$$P_{conv} = \frac{P_{convm}}{31} \left(1 + 20 \frac{I_s}{I_{sm}} + 10 \left(\frac{I_s}{I_{sm}} \right)^2 \right) \quad (10)$$

where P_{convm} is the dissipation in the converter at the rated power, which is assumed to be 3% of the converter's rated power [15]. The rated power of the converter for the reference generator (single double-sided machine) equals the maximum peak power of the plant, namely 1 MW, and the maximum line voltage and phase current are set as 1500 V and 400 A respectively [9].

C. Generator Scaling

The generator is scaled based on the force density (the force acting per unit surface area of the air gap), because it is rather constant for differently sized and designed machines [13]. Two factors are affecting this force density: the air-gap flux density of the stator teeth and the linear current density. The first one is limited by the saturation of magnetic flux and the second one is limited by the maximum allowed heat dissipation. The scale factor of the generator is defined as

$$\lambda = \frac{L_s}{L_o} \quad (11)$$

L_s and L_o represent the stator, translator and stack length of the scaled generator and original generator respectively; subscript 's' and 'o' represent the scaled and original machine. The stator, translator and stack length are scaled together in this work while they are in practice independent sizing parameters. For a fair comparison among generators in various sizes, the maximum allowed stroke and velocity are assumed to be identical. Then other parameters are scaled following:

$$F_{ges} = \lambda^2 F_{geo} \quad (12)$$

$$u_{max_s} = u_{max_o} \quad (13)$$

$$I_{conms} = I_{conmo} \quad (14)$$

$$U_{conms} = \lambda^2 U_{conmo} \quad (15)$$

$$P_s = \lambda^2 P_o \quad (16)$$

where F_{ge} , u_{max} and P represent the rated generator force, maximum floater velocity and power (including rated power of the WEC system and converter). The force density of the reference generator is calculated as 46 kN/m² [9]. In a previous study [3], the maximum required PTO force and optimally economical rated force was calculated as 200 kN and 100 kN respectively for the WEC and sea site considered in this paper. Given the force density, the scale factors are obtained around as 0.5 and 0.7 correspondingly. During the generator scaling, the slot width, pole pitch, number of conductors per slot and magnet pole width remain. It is realized that the lack of design optimization of parameters could not guarantee an optimal performance of the scaled generator. However, the considered scale factor is only varied with a small range between 0.4 to 0.7, which eases the unfairness.

D. Economic Model

An economic model is established to calculate the LCOE of WECs with differently sized generators. The AEP of the generator is calculated as

$$AEP = A \cdot \sum_{x=1}^{x=n} P_{absorbed}(x) \cdot \eta(x) \cdot T(x) \quad (17)$$

where η is the generator efficiency; A is the availability of WECs to work, and it is set as 90% due to necessary operation and maintenance [16]; T represents the total hours of the occurrence of a certain sea state and x means the wave state. The sea site is considered as Yeu island situated in the oceanic territory of France, and its detailed information can be found in [3]. For simplification, the irregular wave states are transferred to regular wave states by equalling their time-averaged power transport per unit length of wave front of incoming waves [3]. The LCOE of a WEC is calculated as

$$LCOE = \frac{CAPEX + \sum_{y=1}^n \frac{OPEX_y}{(1+r)^y}}{\sum_{y=1}^n \frac{AEP_y}{(1+r)^y}} \quad (18)$$

where $CAPEX$ and $OPEX$ are Capital Expenditure ($CAPEX$), and Operational Expenditure ($OPEX$), in which the yearly $OPEX$ is assumed to be 8% of the $CAPEX$; r is the discount rate and assumed as 8% with a lifespan n of 20 years, and Y is the evaluated year [17]. The $CAPEX$ is calculated as

$$CAPEX = C_S + C_F + C_I + C_{PTO} + C_C \quad (19)$$

C_S , C_F , C_I , C_{PTO} and C_C are structure, foundation and mooring, installation, PTO and grid connection costs respectively. The first three terms depend on the structure mass of the WEC which are calculated following the method proposed in [3]. The linear generator costs are calculated as

$$C_{PTO} = 2(C_{Fe}M_{Fe} + C_{Cu}M_{Cu} + C_{pm}M_{pm}) \quad (20)$$

where a factor 2 is considered to include the manufacture cost and converter cost; C_{Fe} , C_{Cu} and C_{pm} are unit price of iron, copper and permanent magnet, and they are assumed to be 3.3 euros/kg, 15.2 euros/kg and 24.7 euros/kg respectively [11]; M_{Fe} , M_{Cu} and M_{pm} are the mass of iron, copper and permanent magnet respectively. The grid connection cost is assumed to be 32% of the PTO cost [3].

IV. RESULTS AND DISCUSSION

A. Generator Performance

Taking one operating point as an example, the performance of the generator with a scaling factor of 0.7 over a half wave period is depicted in Fig. 4. This operating point corresponds to a floater displacement of 1.45 m and wave period of 8.0 s. Due to a partial overlap between the translator and stator, it can be seen that the profile of the root mean square (RMS) of the no-load voltage is not sinusoidal. The current has to be changed correspondingly to obtain the required generator force. Besides, it is seen that the copper losses are higher than the iron losses and converter losses.

B. Influence of sizing on the generator efficiency

Four scaling factors of the linear generator are considered, namely 0.4, 0.5, 0.6 and 0.7. Their efficiency maps are shown in Fig. 5. The generator efficiency is defined as the electrical power delivered to the grid divided by the mechanical power absorbed by the floater. A few null cells are observed in Fig. 5 for the smallest generator at low wave periods and very high wave heights where the floater velocity tends to be high. It results from the conflict between satisfying the force and velocity constraints, and no feasible PTO damping coefficient can be applied. For smaller generators, the PTO force constraint becomes stricter, which is not capable to limit the velocity to the defined constraint. This in practice implies that the device has to be stopped from violating physical limits. Furthermore, when the scale factors are 0.5 and 0.6, a sharp unwarped in the efficiency map is observed along the increase of the wave height especially at long wave periods. This can be explained by the fact that the PTO damping coefficients are reduced from the optimal values in these wave states to satisfy the defined force constraints. The reduced PTO damping coefficient results in a higher floater velocity, in which the no-load voltage increased and the current can thus be lower to generate the required force. As a consequence, the copper losses are decreased and then the generator efficiency is improved. However, this is not necessarily beneficial for the energy production because of the reduced amount of the absorbed mechanical power by the floater.

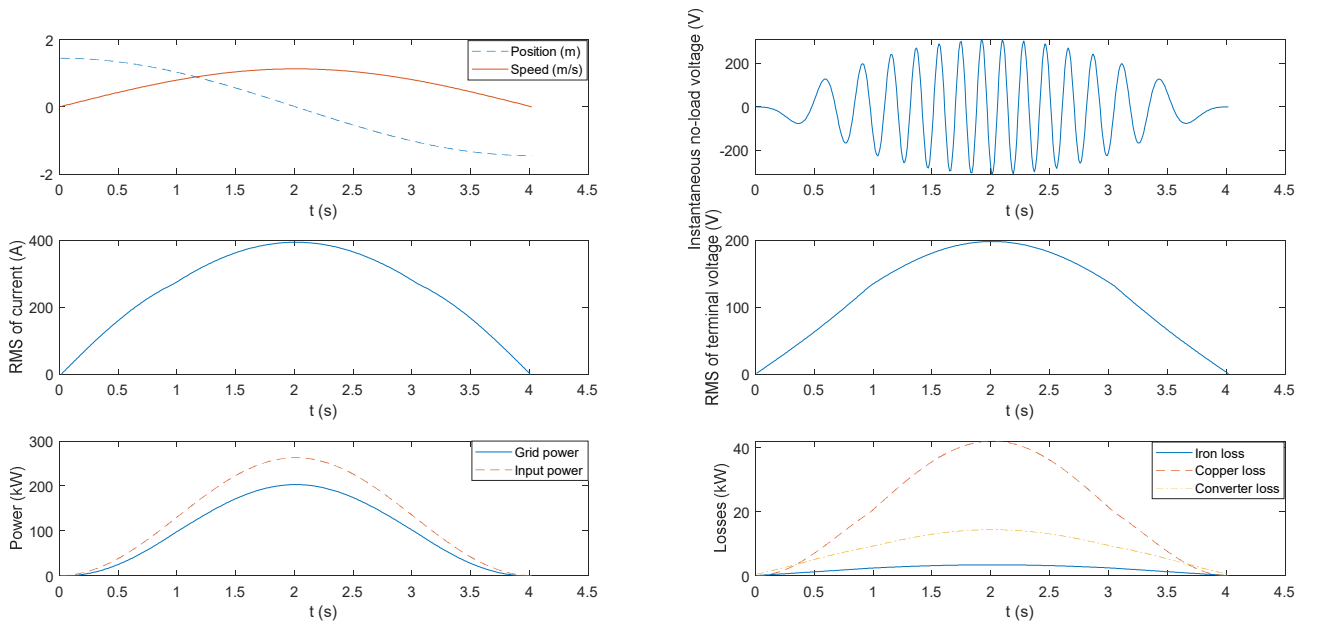


Fig. 4. Generator performance over a half of wave period with a displacement of 1.45 m and a wave period of 8.0 s

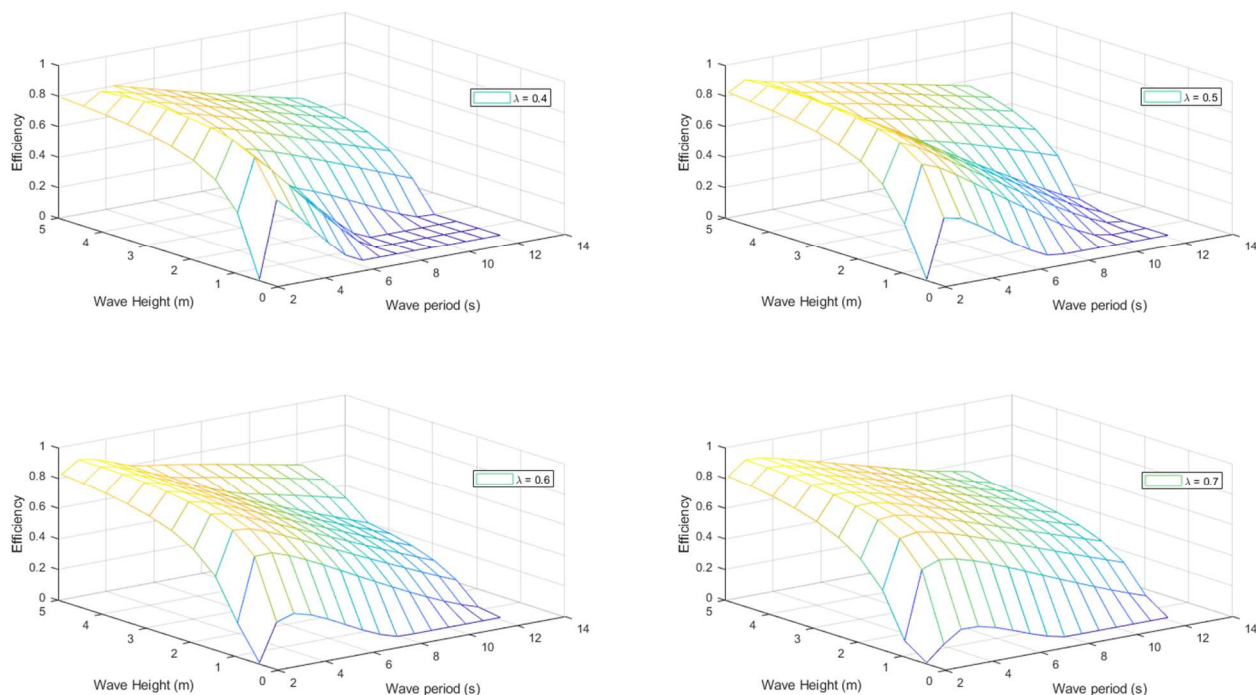


Fig. 5. Generator efficiency maps with different scale factors

It is also seen from Fig. 5 that larger generators have higher efficiencies. In addition, the efficiency generally increases with the wave height and declines with the wave periods. For the small generators (with a scale factor of 0.4 and 0.5), the efficiencies are even around zero at wave states with very low wave heights and long wave periods. Because the no-load voltages at these wave states are very low, and therefore the currents are increased to be remarkably high to generate the required force. In this way, the input mechanical energy is insufficient to cover the losses.

For the given wave location, the average efficiencies of the variously sized generators are presented in TABLE II. The average overall efficiency of the linear generator is defined as the total yearly energy delivered to the grid divided by the total yearly absorbed mechanical energy. The average grid power and losses is defined as yearly grid energy and losses divided by the yearly time. It is acknowledged that the efficiency of the generator is related to the operating conditions, and therefore the average efficiency differs with the wave location. It is seen that the generator size has a significant influence on the average overall efficiency and grid power, and the larger generators are associated with a better generator performance. For instance, the overall efficiency and average grid power can be improved by 26% and 61% through increasing the scale factor from 0.4 to 0.7. The copper losses account for a major proportion of total losses, and increasing the scale factor reduces the average copper losses. This is expected as the current in larger generators is lower to generate the same required force.

In previous studies investigating the scaling of WECs, the impact of sizing on the PTO efficiency is not considered [17], [18]. However, the results given in Fig. 5 and TABLE II indicate the necessity for taking the detailed efficiency map of the resized generator into consideration when performing the systematic scale optimization of WECs.

TABLE II. OVERALL GENERATOR EFFICIENCY AND AVERAGE LOSSES WITH THE SCALE FACTOR

Scaling factor	0.4	0.5	0.6	0.7
Overall efficiency	54.3%	58.3%	63.2%	68.2%
Grid power (kW)	9.30	12.4	13.8	15.0
Copper losses (kW)	5.40	5.60	4.67	3.44
Iron losses (kW)	0.32	0.46	0.64	0.86
Converter losses (kW)	2.16	2.68	2.87	2.88

C. Techno-economic analysis

Fig. 6 shows the resulted AEP with respect to different scale factors. For a comparison, an assumed constant overall efficiency of 70% is considered for generators in all sizes [3]. The AEP in the case with a constant generator efficiency hardly increases after the scale factor is higher than 0.6. Because the occurrence of highly powerful wave states where larger generators are required to absorb more energy is limited. For the case considering detailed generator efficiency maps, the AEP is observed to continuously increase from the scale factor of 0.4 to 0.7. The reason is that the improved generator efficiency still contributes to the AEP even when the scale factor is higher than 0.6, from which the absorbed energy hardly increases though. Fig. 7 shows the resulted LCOE with respect to different scale factors. Downsizing the generator is beneficial for reducing the LCOE although the overall efficiency of the generator is decreased by it. Specifically, the LCOE in this study is reduced by approximately 11% when downsizing the scale factor from 0.7 to 0.5 for this particular sea site.

Furthermore, the assumed constant efficiency of 70% is clearly optimistic for performing PTO downsizing. The results based on the constant efficiency assumption deviate noticeably from that based on the detailed efficiency map,

particularly for small generators. It is noted from Fig. 6 and 7 that the differences are as high as 28% and 31 % for the AEP and LCOE respectively when the scale factor is 0.4. Therefore, it is highly recommended to include the effect of PTO sizing on generator efficiencies for improving the accuracy of estimation on the LCOE and AEP. Besides, the minimal LCOE corresponds to the scale factor of 0.45 and 0.5 for the case with the constant generator efficiency and detailed efficiency map respectively. This means that neglecting the influence of the PTO sizing on the generator efficiencies could lead to a misestimation for the optimal generator size.

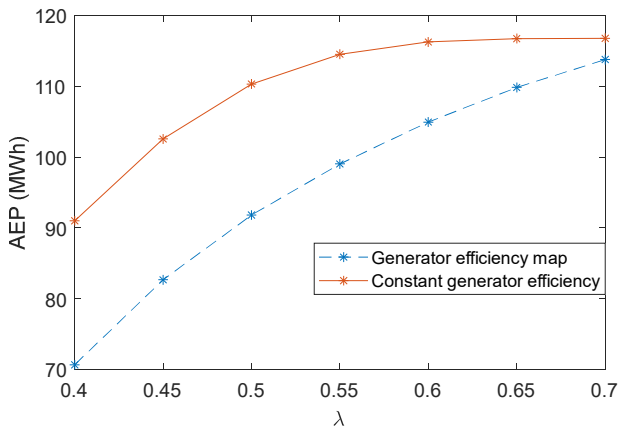


Fig. 6. The AEP as a function of the scale factor of the generator

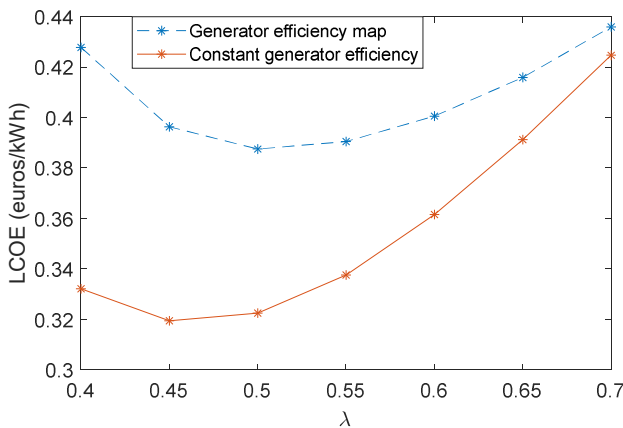


Fig. 7. The LCOE as a function of the scale factor of the generator

V. CONCLUSIONS

The linear PM generators are attractive to act as the PTO systems in WECs due to their high efficiency and reliability. This paper studies the effects of the PTO sizing on generator efficiencies and techno-economic performance of WECs. Both hydrodynamic modelling and generator modelling are presented. The linear PM generator is sized based on the force density for supplying different maximum generator forces. The results show that for the studied sea site, downsizing the generator size to a suitable level reduces the LCOE by 11% even though downsizing is not beneficial for the overall generator efficiency and AEP. In addition, the assumption of a constant generator efficiency leads to an obvious mismatch between the AEP and LCOE estimation with respect to the effect of PTO sizing on the generator efficiency. The difference reaches over 30% for particular

cases. It is highly suggested to consider the detailed efficiency map of the resized generator when performing PTO sizing for WECs.

REFERENCES

- [1] R. Ahamed, K. McKee, and I. Howard, "Advancements of wave energy converters based on power take off (PTO) systems: A review," *Ocean Eng.*, vol. 204, no. March, p. 107248, 2020, doi: 10.1016/j.oceaneng.2020.107248.
- [2] W. Shen *et al.*, "A comprehensive review of variable renewable energy levelized cost of electricity," *Renew. Sustain. Energy Rev.*, vol. 133, no. August, p. 110301, 2020, doi: 10.1016/j.rser.2020.110301.
- [3] J. Tan, H. Polinder, A. J. Laguna, P. Wellens, and S. Miedema, "The Influence of Sizing of Wave Energy Converters on the Techno-Economic Performance," *J. Mar. Sci. Eng.*, vol. 9(1), p. 52, 2021, doi: https://doi.org/10.3390/jmse9010052.
- [4] M. Prado and H. Polinder, *Case study of the Archimedes Wave Swing (AWS) direct drive wave energy pilot plant*. Woodhead Publishing Limited, 2013.
- [5] L. Cappelli *et al.*, "Linear tubular permanent-magnet generators for the inertial sea wave energy converter," *IEEE Trans. Ind. Appl.*, vol. 50, no. 3, pp. 1817–1828, 2014, doi: 10.1109/TIA.2013.2291939.
- [6] M. Eriksson, *Modelling and Experimental Verification of Direct Drive Wave Energy Conversion*. 2007.
- [7] J. K. H. Shek, D. E. Macpherson, and M. A. Mueller, "Experimental verification of linear generator control for direct drive wave energy conversion," *IET Renew. Power Gener.*, vol. 4, no. 5, pp. 395–403, 2010, doi: 10.1049/iet-rpg.2009.0158.
- [8] R. Crozier, H. Bailey, M. Mueller, E. Spooner, and P. McKeever, "Analysis, design and testing of a novel direct-drive wave energy converter system," *IET Renew. Power Gener.*, vol. 7, no. 5, pp. 565–573, 2013, doi: 10.1049/iet-rpg.2012.0072.
- [9] H. Polinder, M. E. C. Damen, and F. Gardner, "Linear PM generator system for wave energy conversion in the AWS," *IEEE Trans. Energy Convers.*, vol. 19, no. 3, pp. 583–589, 2004, doi: 10.1109/TEC.2004.827717.
- [10] M. Prado and H. Polinder, "Direct drive wave energy conversion systems: An introduction," *Electr. Drives Direct Drive Renew. Energy Syst.*, pp. 175–194, 2013, doi: 10.1533/9780857097491.2.175.
- [11] P. Tokat and T. Thiringer, "Sizing of IPM Generator for a Single Point Absorber Type Wave Energy Converter," *IEEE Trans. Energy Convers.*, vol. 33, no. 1, pp. 10–19, 2018, doi: 10.1109/TEC.2017.2741582.
- [12] H. Polinder, M. E. C. Damen, and F. Gardner, "Design, modelling and test results of the AWS PM linear generator," *Eur. Trans. Electr. Power*, vol. 15, no. 3, pp. 245–256, 2005, doi: 10.1002/etep.56.
- [13] H. Polinder, *Principles of electrical design of permanent magnet generators for direct drive renewable energy systems*. Woodhead Publishing Limited, 2013.
- [14] Johannes Falnes, *Ocean waves and Oscillating systems*, vol. 30, no. 7. 2003.
- [15] H. Polinder, F. F. A. Van Der Pijl, G. J. De Vilder, and P. J. Tavner, "Comparison of direct-drive and geared generator concepts for wind turbines," *IEEE Trans. Energy Convers.*, vol. 21, no. 3, pp. 725–733, 2006, doi: 10.1109/TEC.2006.875476.
- [16] M. M. Kramer, L. Marquis, and P. Frigaard, "Performance Evaluation of the Wavestar Prototype," *Proc. 9th Eur. Wave Tidal Conf.*, pp. 5–9, 2011.
- [17] A. de Andres, J. Mailet, J. H. Todalshaug, P. Möller, D. Bould, and H. Jeffrey, "Techno-economic related metrics for a wave energy converters feasibility assessment," *Sustain.*, vol. 8, no. 11, 2016, doi: 10.3390/su8111109.
- [18] A. G. Majidi, B. Bingölbali, A. Akpınar, G. Iglesias, and H. Jafali, "Downscaling wave energy converters for optimum performance in low-energy seas," *Renew. Energy*, vol. 168, pp. 705–722, 2021, doi: 10.1016/j.renene.2020.12.092.